Journal of Natural Disaster Science, Volume 37, Number 2, 2016, pp49-64

Model for forecasting expressway surface temperature in snowy areas

Masafumi Horii* and Takayuki Hayami**

* Department of Civil Engineering, College of Engineering, Nihon University
** Saku Office, Nexco-Maintenance Kanto Company Ltd.

(Received: May. 20, 2016 Accepted :Sept. 28, 2016)

ABSTRACT

We proposed a forecast model that uses a neural network to predict what the winter road surface temperature will be after three hours in order to increase the efficiency of anti-icing programs. In order to establish the forecast model, learning models of the road surface temperature using three sets of input variables at a specific site were created. These learning models were then applied to other sites along an expressway, and the correct classification of the road surface temperature was examined. The results of the present study revealed that the road surface temperature along an expressway can be predicted three hours in advance more than 76% of the time by applying a learning model to the time series variation of the road surface temperature and other variables, such as the hourly traffic volume and the effect of spreading anti-icing chemicals.

Keywords: forecast of road surface temperature, neural network, discriminant analysis

1. Introduction

In snowy areas, highway maintenance authorities often spread chemicals such as sodium chloride (salt) on the road surface in order to increase safety during winter conditions. However, these chemicals damage the soil, plants, vehicles, and roadside structures. The amount of salt used has increased yearly, increasing the financial burden for these services. Therefore, a forecast model of the road surface temperature that enables salt to be spread before the road surface freezes would be beneficial. The model should be simple and easy to apply in daily route-based road maintenance using only existing basic sensor measurements. However, no such practical forecast model has been established.

Several studies on forecast models of the road surface temperature have been conducted. These studies can be classified into two types: 1) methods using heat balance models and 2) statistical methods. Heat balance models have been reported by Rayer (1987), Shao et al. (1993), and Voldborg (1993), and these models have improved the accuracy of the road surface temperature prediction. However, these models are difficult to apply in all locations for which effective winter road maintenance is needed because they require several types of equipment for the observation of meteorological variables, such as solar radiation, radiation balance, and albedo.

With respect to statistical methods, Suzuki et al. (1993) constructed a forecast model of the road surface temperature that uses multiple regression analysis and reported that a fairly accurate forecast model could be obtained. Shao (1998) and Almkvist and Walter (2006) investigated the forecasting of the road surface temperature using a neural network model. These methods also require several types of equipment for measuring meteorological variables.

Under these conditions, we proposed a forecast model that uses a neural network to predict road surface temperatures three hours in advance at a specific site on an expressway based on measurements

using existing basic sensors and obtained acceptably accurate results. Moreover, we confirmed that the neural network model has an accuracy similar to that of multiple regression models (Suzuki et al., 1993) by comparing the results (Horii and Fukuda, 2000). Furthermore, Horii (2013) applied a forecast model to sites on a national highway and established a route-based forecast model having sufficient accuracy for practical application. In our previous studies, we constructed the model by inputting the times series data for only one variable, that is, road surface temperature. In the present paper, however, we apply the proposed model (Horii, 2013) to an expressway by changing the input variables. We examine the effect of the input variables of the forecast model and evaluate the difference in precision between the various sets of input variables of the route-based model in order to increase the efficiency of anti-icing programs (Horii and Hayami, 2015).

2. Forecast model

Artificial neural networks are computer models that are inspired by components of the human brain and are powerful tools that can be used to solve complex problems. The neural network used in the present study is a multilayer network, as shown in Fig. 1. A neural network consists of three layers: an input layer, a hidden layer, and an output layer. The input neurons receive signals from outside the model and send their outputs to the hidden neurons. The output neurons receive signals from the hidden neurons and produce the final outputs.

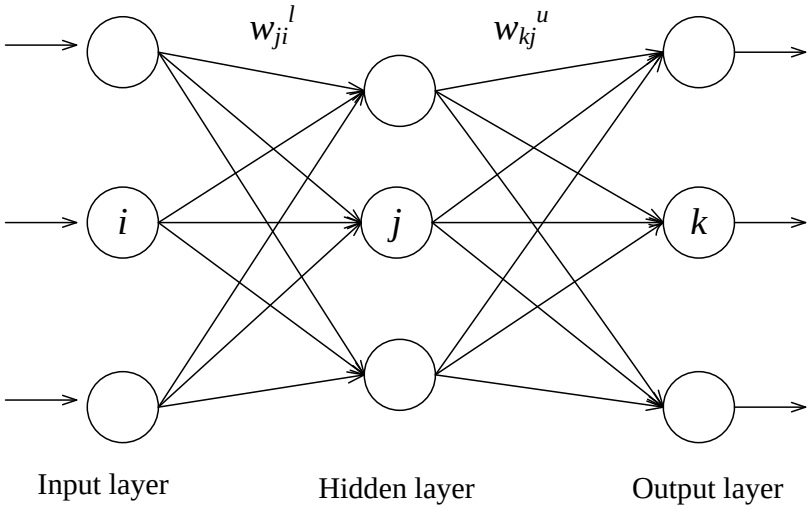

Figure 1. Multilayered neural network

The outputs of the hidden and output neurons, denoted by o_j and y_k, respectively, are given by

$$o_j = f(u_j) = f\left(\sum_{i=1}^{I} w_{ji}^{l} x_i \right) \qquad (1)$$

$$y_k = f(z_k) = f\left(\sum_{j=1}^{J} w_{kj}^{u} o_j \right) \qquad (2)$$

where u_j is the input to the jth neuron in the hidden layer, z_k is the input to the kth neuron in the output layer, w_{ji}^{l} is the connection weight between the jth neuron in the hidden layer and the ith neuron in the input layer,

w_{kj}^{u} is the connection weight between the kth neuron in the output layer and the jth neuron in the hidden layer, x_i is the input to the ith neuron in the input layer, and I and J are the numbers of neurons in the input and the hidden layer, respectively. The most commonly used activation function is a sigmoid function:

$$f(x)=\frac{1}{1+e^{-x}} \qquad (3)$$

Neural networks can be trained by adjusting the connection weights in order to abstract the relationships between the input data and the output data. This learning procedure can be achieved by minimizing the error between the desired outputs and the actual outputs:

$$E=\frac{1}{2}\sum_{k=1}^{K}(y_k-y_{dk})^2 \qquad (4)$$

where y_{dk} is the desired output signal of the kth neuron in the output layer, and K is the number of neurons in the output layer. In general, the error backpropagation algorithm is applied in order to minimize this error function. However, the backpropagation learning algorithm has some problems. The backpropagation process requires too many learning cycles to converge to the correct weights, and the learning process becomes stuck at a local minimum of the error.

In the present paper, a learning algorithm that is based on an extended Kalman filter has been introduced (Murase et al., 1994). We assume the following nonlinear state model (Katayama, 1983):

$$w_{t+1}=f_t(w_t)+v_t \qquad (5)$$

$$y_t=h_t(w_t)+n_t \qquad (6)$$

where w_t is the n-dimensional state vector at time t, y_t is the p-dimensional observation vector, $f_t(w_t)$ and $h_t(w_t)$ are the n- and p-dimensional nonlinear vector functions, respectively, v_t is the zero-mean m-dimensional plant noise, and n_t is the zero-mean p-dimensional observation noise with covariance matrices

$$E\left\{\begin{pmatrix}v_t\\ n_t\end{pmatrix}\begin{pmatrix}v_\tau^{\,T} & n_\tau^{\,T}\end{pmatrix}\right\}=\begin{bmatrix}Q_t & 0\\ 0 & R_t\end{bmatrix}\delta_{t\tau} \qquad (7)$$

in which Q_t is a matrix of size $m \times m$, R_t is a matrix of size $p \times p$, and $\delta_{t\tau}$ is the Kronecker delta.

Here, since the connection weights are the elements of the state vector and are assumed to be time invariant, the plant noise is not taken into consideration. Therefore, in place of Equation 5, the state equation can be expressed as follows:

$$w_{t+1}=Iw_t \qquad (8)$$

where I is the identity matrix.

Since $h_t(w_t)$ is a nonlinear function, this function is linearized around the estimate of the state as follows:

$$h_t(w_t)=h_t(\hat{w}_{t/t-1})+H_t(w_t-\hat{w}_{t/t-1}) \qquad (9)$$

Then, an extended Kalman filter algorithm can be applied to the estimates of the states. By substituting Equation 9 into Equation 6, we can derive the following expression to replace Equation 6:

$$\eta_t = H_t w_t + n_t \qquad (10)$$

where

$$\eta_t = y_t - h_t(\hat{w}_{t/t-1}) + H_t \hat{w}_{t/t-1} \qquad (11)$$

and H_t is the gradient matrix that results from linearizing the network and is defined as follows:

$$H_t = \left(\frac{\partial h_t}{\partial w_t} \right)_{w=\hat{w}_{t/t-1}} \qquad (12)$$

Using the state and observation equations, a method for updating the estimators of the system can be derived. The updated equations are

$$\hat{w}_{t/t} = \hat{w}_{t/t-1} + K_t \left[y_t - h_t \left(\hat{w}_{t/t-1} \right) \right] \qquad (13)$$

$$\hat{w}_{t+1/t} = \hat{w}_{t/t} \qquad (14)$$

$$K_t = P_{t/t-1} H_t^T \left(H_t P_{t/t-1} H_t^T + R_t \right)^{-1} \qquad (15)$$

$$P_{t/t} = P_{t/t-1} - K_t H_t P_{t/t-1} \qquad (16)$$

$$P_{t+1/t} = P_{t/t} \qquad (17)$$

where $\hat{w}_{t/t}$ is the Kalman filter estimate of the state at time t based on its one-step prediction, K_t is the Kalman gain, and $P_{t/t}$ is an estimation error covariance matrix.

3. Application

3.1. Learning model of road surface temperature

We applied a neural network model based on the extended Kalman filter to forecast road surface temperatures at three sites of the Ban-Etsu expressway in Fukushima prefecture. Site A (99.1 kp, altitude: 512.6 meters) and Site C (121.5 kp, altitude: 190.4 meters) are located in embankment sections, and Site B (105.3 kp, altitude: 570.8 meters) is located in a cut section. Here, kp refers to kilo-posts and indicates the distance from the origin of a route.

Observation data from December 2013 to March 2014 were provided by the Tohoku Regional Head Office of the East Nippon Expressway Company (NEXCO East, 2013-2014). These data consist of air temperature, road surface temperature, temperatures at 5 and 10 centimeters underground, wind velocity, amounts of rainfall and snowfall per hour, traffic volume, and reports on operations of spreading anti-icing chemicals. Furthermore, the grid point value (GPV) data at the nearest point of three sites at 37.6 degrees north latitude and 140.0 degrees east longitude were collected. The GPV data were provided by the Japan Meteorological Agency and were calculated using the Global Spectral Model.

The model structure is a three-layer network, as shown in Fig. 2. We used the time series variation of data as inputs to the input neurons and the road surface temperatures after three hours as outputs to the output neurons. Three hours corresponds to the amount of time required for a salt spreader to depart from a snow removal station and complete the spreading operation.

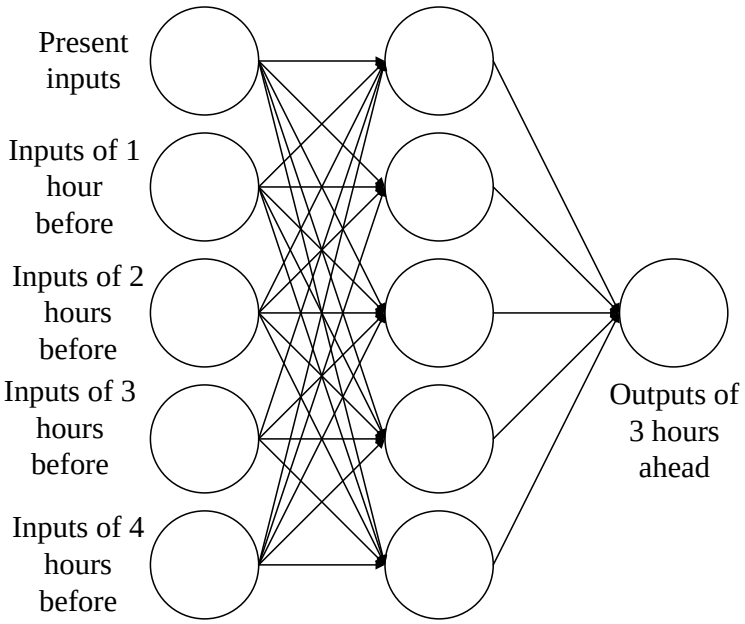

Figure 2. Basic architecture for forecasting road surface temperatures

In the present paper, we selected three sets of input variables: 1) road surface temperature, 2) road surface temperature, hourly traffic volume, and effectiveness of spreading anti-icing chemicals, and 3) selected variables by stepwise discriminant analysis. The stepwise discriminant analysis for variable was carried out by adding and deleting variables from the equation according to the partial *F* values in order to find the appropriate discriminant equation. Refer to, for example, Afifi and Clark (1984) for details. Here, the data on the effectiveness of spreading anti-icing chemicals can be represented by a dummy variable that takes one of two values: 1, indicating chemicals on a road surface are effective, and 0, indicating otherwise. We assume anti-icing chemicals on a road surface to be effective for three hours after salt spreader operation.

The selection of the model structure was based on the learning and testing results. Here, the data set for learning was a period of 31 days, from January 1 to January 31 of 2014, and the data set for testing was a period of 90 days, from December 1 to December 31 of 2013 and from February 1 to March 31 of 2014. Firstly, we constructed the learning model by varying the input neurons and hidden neurons for each input variable. We then predicted the outputs of these models using the testing data set, which had not been previously presented to the models. Finally, we decided the forecast model structure of the road surface temperature with the best classification results of the learning and testing. The number of iterations for learning was fixed at 100, for the sake of practicality (Horii and Fukuda, 2000).

At the same time, discriminant analysis was used to examine whether the road surface temperatures could be adequately predicted by the neural network model. Discriminant analysis was used to assign a new sample belonging to two or more groups in order to minimize the probability of misclassification.

Evaluation of the classification results was conducted in terms of 1) total correct classification, including correct classification of the road surface temperatures for above-zero and below-zero conditions, and 2) critical correct classification for dangerous road conditions, that is, below-zero road surface temperatures.

Tables 1 and 2 show the best results of the correct classification for the learning and testing data obtained using the first set of input variables at Site A. In this case, the input variables are the time series

variation of the road surface temperature for six hours, and the number of hidden neurons is nine. Tables 3 and 4 show the same results obtained using the second set of input variables, which are the time series variation of the road surface temperature for six hours, the hourly traffic volume, and the effectiveness of spreading anti-icing chemicals for three hours, at Site A. The number of hidden neurons in this case is again nine. In both cases, the percentages of overall correct classification for the learning and testing data were high: 88.4% (first set, learning), 84.1% (first set, testing), 89.2% (second set, learning), and 77.6%. (second set, testing).

Table 1. Learning results for road surface temperature using the first set of input variables (January of 2014, Site A).

Measured conditions	Predicted conditions		Correct classification
	Below zero	Above zero	
Below zero	496	38	92.9%
Above zero	46	145	75.9%
Correct classification	91.5%	79.2%	88.4%

Table 2. Tasting results for road surface temperature using the first set of input variables (Other three months, Site A).

Measured conditions	Predicted conditions		Correct classification
	Below zero	Above zero	
Below zero	964	123	88.7%
Above zero	213	815	79.3%
Correct classification	81.9%	86.9%	84.1%

Table 3. Learning results for road surface temperature using the second set of input variables (January of 2014, Site A).

Measured conditions	Predicted conditions		Correct classification
	Below zero	Above zero	
Below zero	496	38	92.9%
Above zero	40	151	79.1%
Correct classification	92.5%	79.9%	89.2%

Table 4. Tasting results for road surface temperature using the second set of input variables (Other three months, Site A).

Measured conditions	Predicted conditions		Correct classification
	Below zero	Above zero	
Below zero	982	105	90.3%
Above zero	368	660	64.2%
Correct classification	72.7%	86.3%	77.6%

Table 5 shows the discriminant functions for two groups of data: data for below-zero road surface temperatures and data for above-zero road surface temperatures. The predictor variables in this table were selected based on the results of the stepwise discriminant analysis. A new sample is assigned to the group with the higher discriminant function score.

Table 5. Discriminant functions

Predictor variables	Coefficients of discriminant functions		Partial F value
	Below zero	Above zero	
Road surface temperature	-0.209	0.727	1275.7
Hourly traffic volume	0.017	0.030	708.3
Surface temperature (GPV)	-1.037	-0.710	496.0
Relative humidity at 500 hPa (GPV)	0.089	0.077	374.5
Constant	-5.127	-6.536	

Tables 6 and 7 show the results of correct classification for the learning and testing data obtained using the third set of input variables, which consists of the time series variation of the road surface temperature for eight hours, the hourly traffic volume for three hours, the surface temperature for two hours, and the relative humidity at 500 hPa for one hour, all at Site A. In this case, the number of hidden neurons is seven. We obtained fairly high percentages of overall correct classification for the learning (93.4%) and testing data (84.7%). The three forecast model structures are summarized in Table 8.

Table 6. Learning results for road surface temperature using the third set of input variables (January of 2014, Site A).

Measured conditions	Predicted conditions		Correct classification
	Below zero	Above zero	
Below zero	502	32	94.0%
Above zero	16	175	91.6%
Correct classification	96.9%	84.5%	93.4%

Table 7. Tasting results for road surface temperature using the third set of input variables (Other three months, Site A).

Measured conditions	Predicted conditions		Correct classification
	Below zero	Above zero	
Below zero	933	154	85.8%
Above zero	169	859	83.6%
Correct classification	84.7%	84.8%	84.7%

Table 8. Summary of forecast model structures

Set No. of input variables	Input neurons		Number of hidden neurons
	Variable name	hours	
First set	Road surface temperature	6	9
Second set	Road surface temperature Hourly traffic volume Spreading results of anti-icing chemicals	6 3 3	9
Third set	Road surface temperature Hourly traffic volume Surface temperature (GPV) Relative humidity at 500 hPa (GPV)	8 3 2 1	7

Figures 3 and 4 show the learning and testing results, respectively, obtained using the first set of input variables for Site A. Figures 5 and 6 show the same results obtained using the second set of input variables, and Figs. 7 and 8 show the same results obtained using the third set of input variables. In every case, the predicted values follow the observed values. Therefore, we can obtain three models that enable high-precision learning and testing.

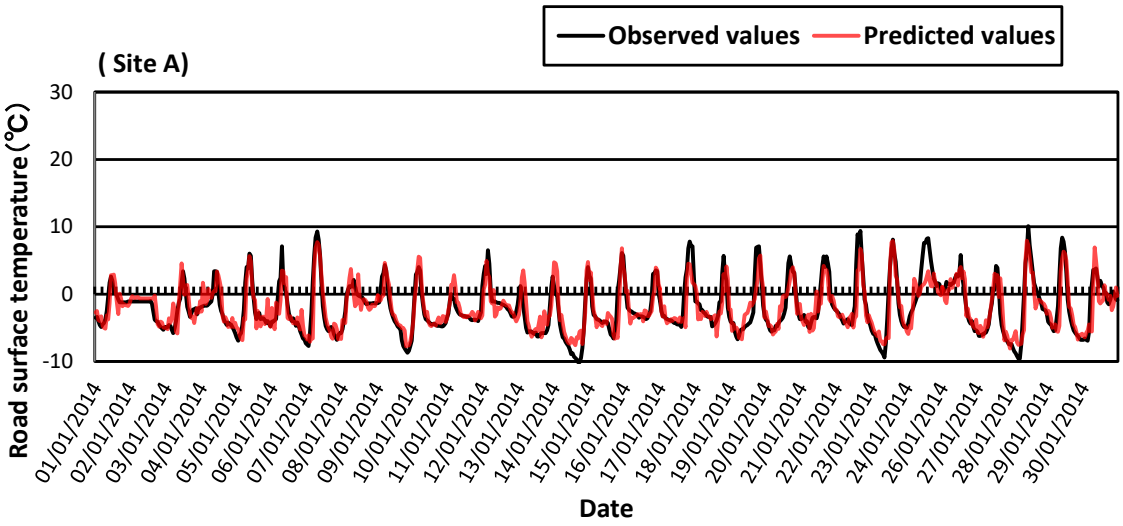

Figure 3. Learning results for road surface temperatures using the first set of input variables (December of 2014, Site A)

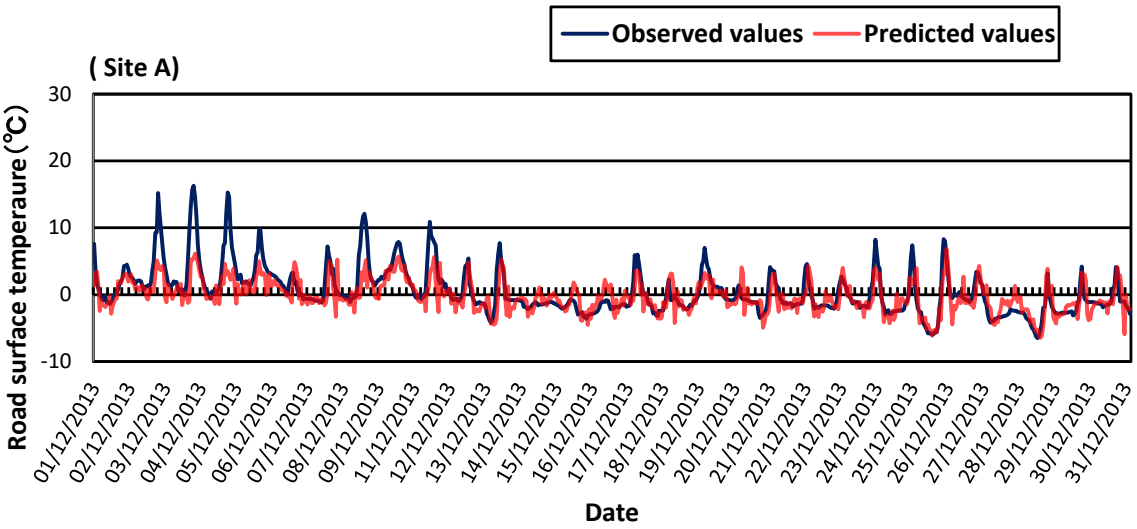

Figure 4. Testing results for road surface temperatures using the first set of input variables (December of 2013, Site A)

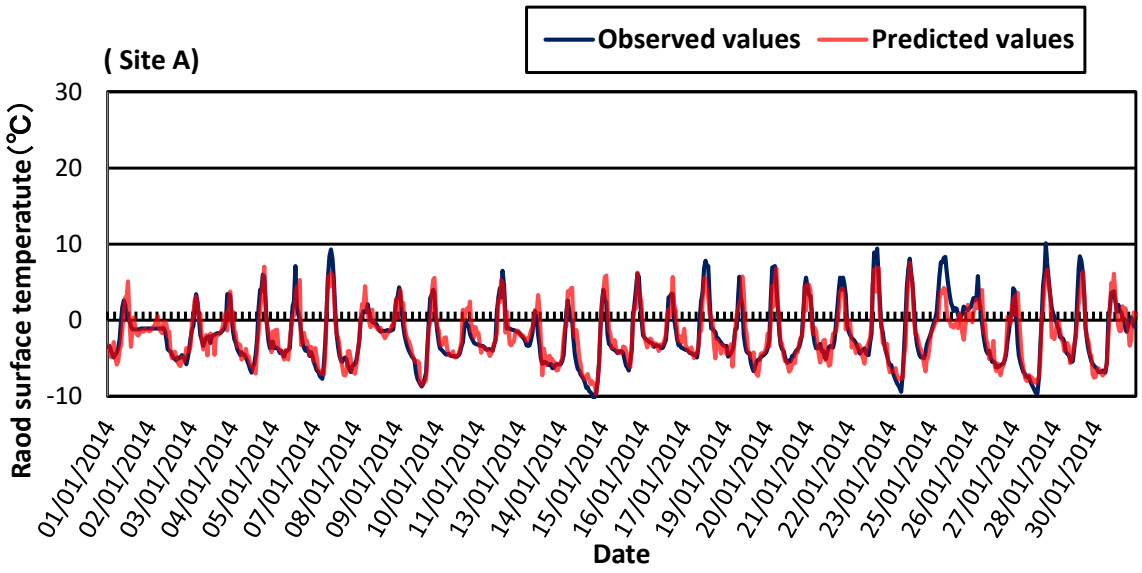

Figure 5. Learning results for road surface temperatures using the second set of input variables (January of 2014, Site A)

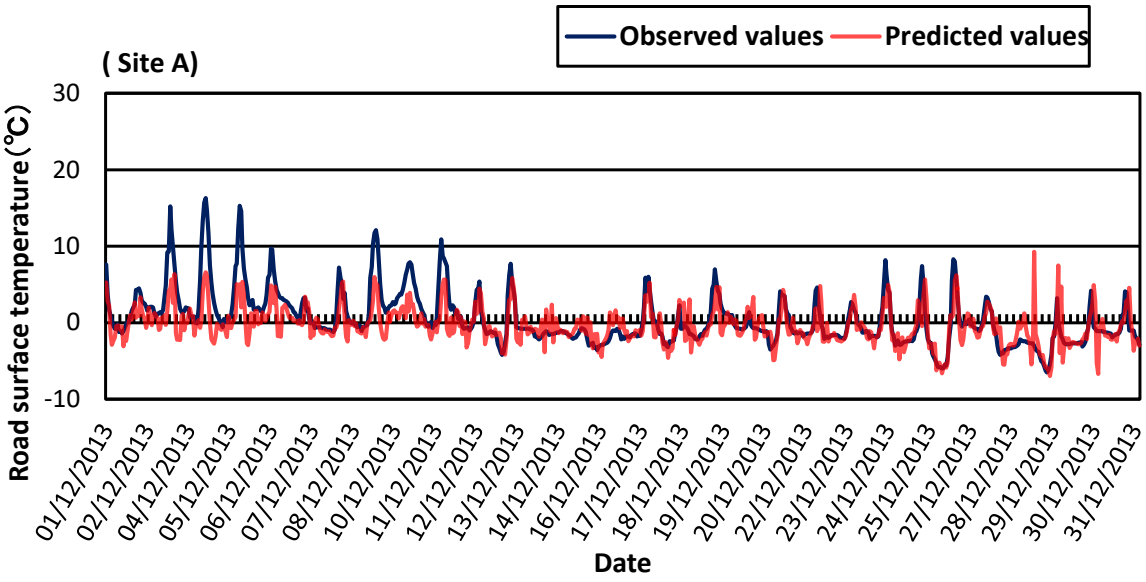

Figure 6. Testing results for road surface temperatures using the second set of input variables (December of 2013, Site A)

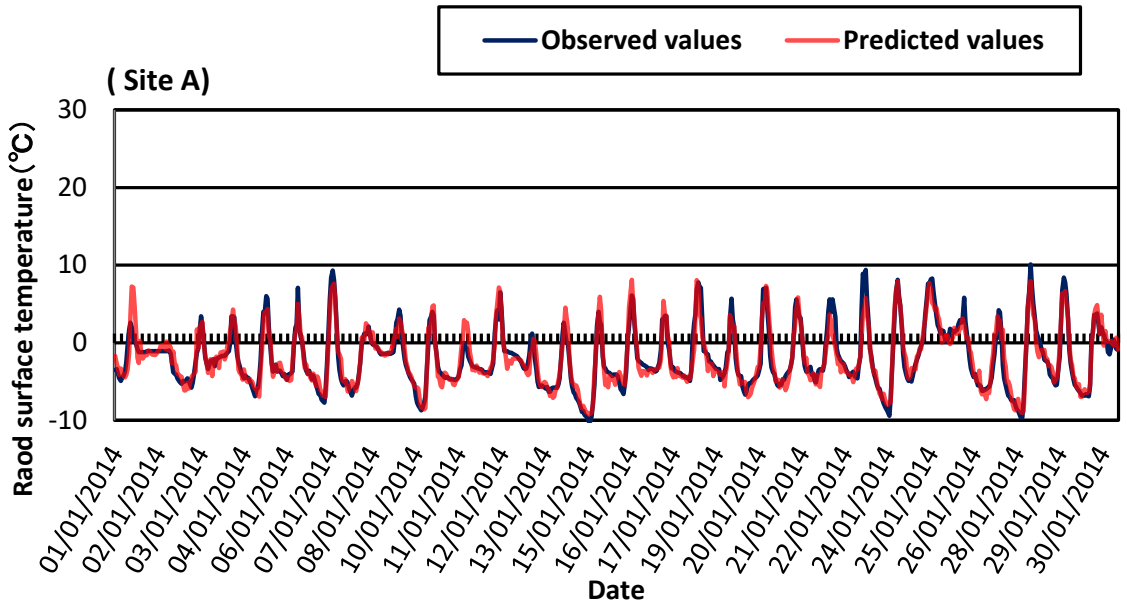

Figure 7. Learning results for road surface temperatures using the third set of input variables (January of 2014, Site A)

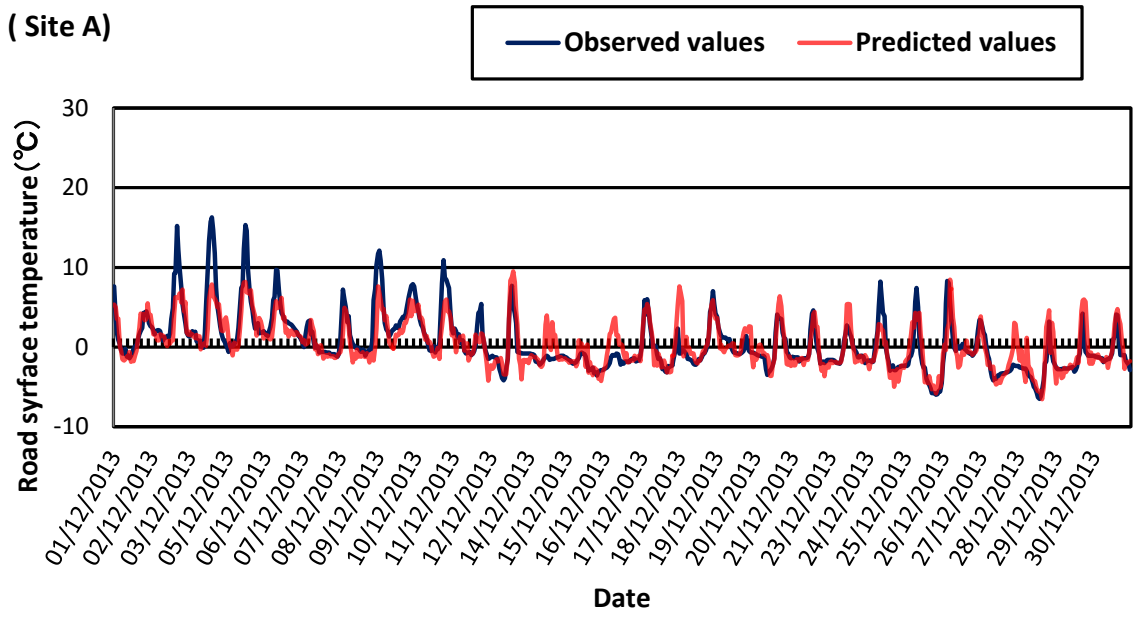

Figure 8. Testing results for road surface temperatures using the third set of input variables (December of 2013, Site A)

3.2. Forecasting road surface temperature for other sites along the expressway

Next, we examined the possibility of forecasting road surface temperatures at other sites along the expressway using the learning model of the road surface temperature at Site A (99.1 kp).

Tables 9, 10, and 11 show the forecast results obtained using the time series variation of the first, second, and third sets of input variables, respectively, at Site B, which is located 6.2 kilometers from Site A. Tables 12, 13, and 14 show the same results for Site C, which is located 22.4 kilometers from Site A. For the two sites, the percentages of critical correct classification results obtained using the first set of input variables and the third set of input variables were 94.5% (Site B, first set), 93.3% (Site B, third set), 89.6% (Site C, first set), and 91.0% (Site C, third set), which are extremely high for below-zero conditions. Furthermore, the percentages of correct classification results obtained using the second set of input variables were 85.6% (Site B, second set) and 86.4% (Site C, second set). These percentages are considerably high for overall prediction. Therefore, when considering the correct classification for overall prediction, we should use the second set of input variables, and when considering the correct classification for critical condition, that is, below-zero road surface temperatures, we should use the first or third set of input variables. Thus, the expressway maintenance authorities would select the forecast model according to the traffic volume, weather conditions, and financial burden for these services.

Table 9. Forecast results for road surface temperature using the first set of input variables (four months, Site B).

Measured conditions	Predicted conditions		Correct classification
	Below zero	Above zero	
Below zero	1299	76	94.5%
Above zero	456	1009	68.9%
Correct classification	74.0%	93.0%	81.3%

Table 10. Forecast results for road surface temperature using the second set of input variables (four months, Site B).

Measured conditions	Predicted conditions		Correct classification
	Below zero	Above zero	
Below zero	1160	215	84.4%
Above zero	194	1271	86.8%
Correct classification	85.7%	85.5%	85.6%

Table 11. Forecast results for road surface temperature using the third set of input variables (four months, Site B).

Measured conditions	Predicted conditions		Correct classification
	Below zero	Above zero	
Below zero	1283	92	93.3%
Above zero	585	1191	60.1%
Correct classification	68.7%	90.5%	76.2%

Table 12. Forecast results for road surface temperature using the first set of input variables (four months, Site C).

Measured conditions	Predicted conditions		Correct classification
	Below zero	Above zero	
Below zero	972	113	89.6%
Above zero	420	1335	76.1%
Correct classification	69.8%	92.2%	81.2%

Table 13. Forecast results for road surface temperature using the second set of input variables (four months, Site C).

Measured conditions	Predicted conditions		Correct classification
	Below zero	Above zero	
Below zero	888	197	81.8%
Above zero	189	18566	89.2%
Correct classification	82.5%	88.8%	86.4%

Table 14. Forecast results for road surface temperature using the third set of input variables (four months, Site C).

Measured conditions	Predicted conditions		Correct classification
	Below zero	Above zero	
Below zero	987	98	91.0%
Above zero	565	1190	67.8%
Correct classification	63.6%	92.4%	76.7%

Figures 9 and 10 show the forecast results for the road surface temperature at Sites B and C obtained using the learning model for Site A and the observations of time series variation of the third set of input variables at Sites B and C, which has extremely high percentages of correct classification for below-zero conditions. In both cases, the predicted road surface temperatures follow the observed values for near-zero conditions. In contrast, larger errors occur at higher road surface temperatures. However, this is not problematic, because this temperature range is not subject to ice formation.

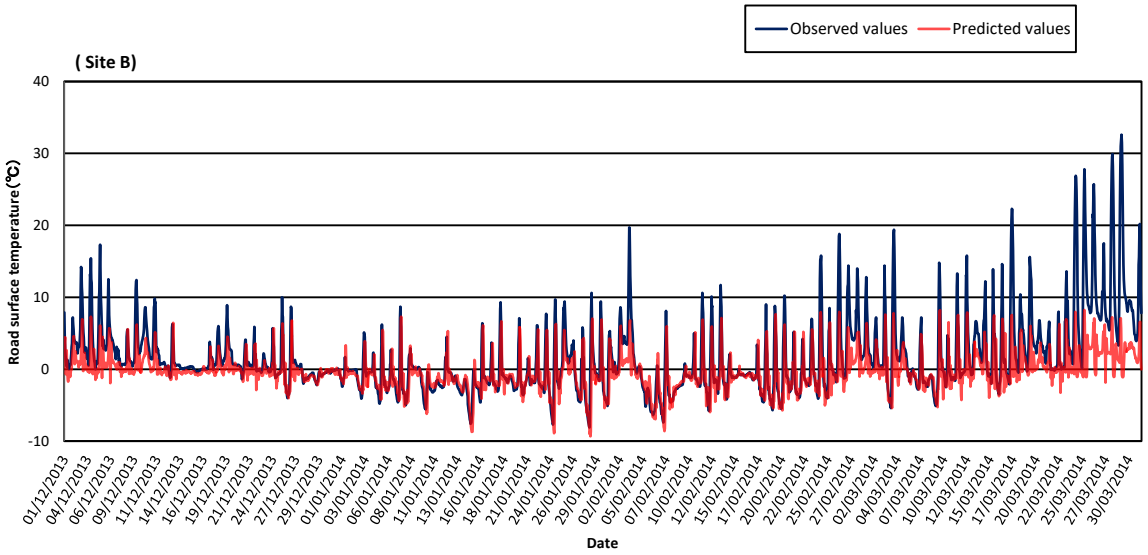

Figure 9. Forecast results for road surface temperature using the third set of input variables (four months, Site B).

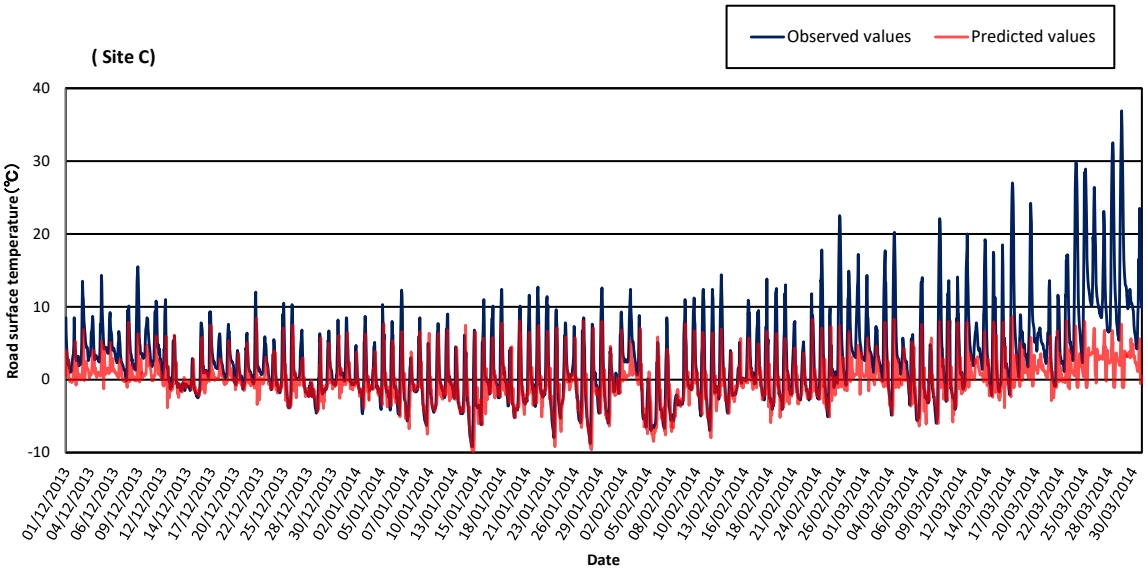

Figure 10. Forecast results for road surface temperature using the third set of input variables (four months, Site C).

4. Conclusion

In the present paper, we attempted to establish a forecast model of the road surface temperature along an expressway.
The results are as follows:
1. The neural network model has the ability to forecast road surface temperature with high precision.
2. We examined the ability of the learning model to forecast the road surface temperature at other sites along the expressway, i.e., route-based forecasting of the road surface temperature.
3. We obtained three models that have the ability to forecast road surface temperatures for overall conditions or road surface temperatures in below-zero conditions along the expressway using different input variables.

For expressway maintenance in winter, it is of particular importance to carefully maintain safe road surface conditions by using an appropriate forecast model of the road surface temperature when below-zero conditions might exist.

We hope to establish a route-based forecast model for the road surface conditions by combining the proposed model and a model for detecting water on road surfaces. This model uses a discriminant analysis and a neural network to predict dry versus other road surface conditions three hours in advance (Horii and Fukuda, 2001).

Acknowledgments

The present research was supported in part by a Grant from the Ministry of Education, Culture, Sports, Science, and Technology (No. 26350490). We are grateful to the staff of Koriyama and Aizu Office of East Nippon Expressway Company.

REFERENCES

Afifi, A. A. and Clark, V., 1984. Computer-aided multivariate analysis, Lifetime Learning Publication.
Almkvist, S. E. and Walter, M., 2006. Which variables should be measured at a road weather station –

Artificial intelligence gives the answer, SIRWEC, 101-107.
Horii, M. and Fukuda, T., 2000. Forecast model of road surface temperature in snowy areas using neural network, Proceedings of the Fourth International Conference on Snow Engineering, 403-407.
Horii, M. and Fukuda, T., 2001. Pavement ice prediction system in winter maintenance, Journal of Materials, Concrete Structures and Pavements, 669, 243-251.
Horii, M., 2013. Forecast model of road surface temperature along national highway in snowy area, Journal of Snow Engineering of Japan, 29 (1), 13-22.
Horii, M. and Hayami, T., 2015. Forecast model of road surface temperature along expressway, Summaries of JSSI & JSSE Joint Conf. on Snow and Ice Research, 99.
Katayama, T., 1983. Applied Kalman Filter, Asakura Publishing Co., Ltd.
Murase, H., Koyama, S., and Ishida, R., 1994. Kalman neuro computing by personal computer, Morikita Publishing Co., Ltd.
NEXCO East, 2013-2014. Meteorological and Traffic Survey Data.
Rayer, P. J., 1987. The Meteorological Office forecast road surface temperature model, Meteorological Magazine, 116, 180-191.
Shao, J., Thornes, J. E., and Lister, P. J., 1993. Description and verification of a road ice prediction model, Transportation Research Record, 1387, 216-222.
Shao, J., 1998. Improving nowcasts of road surface temperature by a backpropagation neural network, Weather and Forecasting, 13, 164-171.
Suzuki, T., Amano, T., and Hirama, S., 1993. Research on new system for prediction freezing on road surfaces, Report of Research Center of Japan Highway Public Corporation, Vol. 30, 179-190.
Voldborg, H., 1993. On the prediction of road conditions by a combined road layer-atmospheric model in winter, Transportation Research Record, 1387, 231-235.